Journal of Structural Geology, Vol. 13, No. 10, pp. 1157 to 1171, 1991
Printed in Great Britain

0191-8141/91 $03.00+0.00

Discrete Proterozoic structural terranes associated with low-*P*, high-*T* metamorphism, Anmatjira Range, Arunta Inlier, central Australia: tectonic implications

W. J. COLLINS

Department of Geology, University of Newcastle, Newcastle, NSW 2308, Australia

R. H. VERNON and G. L. CLARKE*

School of Earth Sciences, Macquarie University, Sydney, NSW 2109, Australia

(*Received* 12 *May* 1989; *accepted in revised form* 9 *May* 1991)

Abstract—Structural overprinting relationships indicate that two discrete terranes, Mt. Stafford and Weldon, occur in the Anmatjira Range, northern Arunta Inlier, central Australia. In the Mt. Stafford terrane, early recumbent structures associated with $D_{1a,1b}$ deformation are restricted to areas of granulite facies metamorphism and are overprinted by upright, km-scale folds (F_{1c}), which extend into areas of lower metamorphic grade. Structural relationships are simple in the low-grade rocks, but complex and variable in higher grade equivalents. The three deformation events in the Mt. Stafford terrane constitute the first tectonic cycle (D_1). D_2 deformation in the Weldon terrane comprises the second tectonic cycle. The earliest foliation (S_{2a}) was largely obliterated by the dominant reclined to recumbent mylonitic foliation (S_{2b}), produced during progressive non-coaxial deformation, with local sheath folds and W- to SW-directed thrusts. Locally, D_{2b} tectonites have been rotated by N–S-trending, upright F_{2c} folds, but the regional upright fold event (F_{2d}), also evident in the adjacent Reynolds Range, rotated earlier surfaces into shallow-plunging, NW–SE-trending folds that dominate the regional outcrop pattern.

The terranes can be separated on structural, metamorphic and isotopic criteria. A high-strain D_2 mylonite zone, produced during W- to SW-directed thrusting, separates the Weldon and Mt. Stafford terranes. 1820 Ma megacrystic granites in the Mt. Stafford terrane intruded high-grade metamorphic rocks that had undergone D_{1a} and D_{1b} deformation, but in turn were deformed by S_{1c}, which provides a minimum age limit for the first structural–metamorphic event. 1760 Ma charnockites in the Weldon terrane were emplaced post-D_{2a}, and metamorphosed under granulite facies conditions during D_{2b}, constraining the second tectonic cycle to this period.

Each terrane is associated with low-*P*, high-*T* metamorphism, characterized by anticlockwise *P–T–t* paths, with the thermal peaks occurring before or very early in the tectonic cycle. These relations are not compatible with continental-style collision, nor with extensional tectonics as the deformation was compressional. The preferred model involves thickening of previously thinned lithosphere, at a stage significantly after (>50 Ma) the early extensional event. Compression was driven by external forces such as plate convergence, but deformation was largely confined to and around composite granitoid sheets in the mid-crust. The sheets comprise up to 80% of the terranes and induced low-*P*, high-*T* metamorphism, including migmatization, thereby markedly reducing the yield strength and accelerating deformation of the country rocks. Mid-crustal ductile shearing and reclined to recumbent folding resulted, followed by upright folding that extended beyond the thermal anomaly. Thus, thermal softening induced by heat-focusing is capable of generating discrete structural terranes characterized by subhorizontal ductile shear in the mid-crust, localized around large granitoid intrusions.

INTRODUCTION

MANY Proterozoic fold belts are characterized by high-grade recumbent mylonitic foliations produced by ductile shear at mid- to deep-crustal levels, during granulite facies metamorphism. These fabrics can sometimes be related to continental-style collision (e.g. Park 1981), particularly where transport directions are constant over large areas, as in the Grenville Province (Moore *et al.* 1986). However, the prograde *P–T–t* paths are commonly anticlockwise, and indicate isobaric cooling associated with compression; examples include the Broken Hill Block (Phillips & Wall 1981), the Olary Block (Clarke *et al.* 1987) and the East Antarctic Shield (Clarke *et al.* 1989b, Stüwe & Powell 1989a,b). These *P–T–t* paths are incompatible with mountain-building processes and alternative explanations include extension of normally-thickened crust (e.g. Wickham & Oxburgh 1985) or collapse of overthickened crust, produced earlier by either tectonic accretion (Sandiford 1989) or magmatic underplating (Stüwe & Powell 1989b). None of these models explains the abnormally high geotherms existing prior to, or synchronous with, compressional deformation in the Proterozoic northern Arunta Inlier, central Australia (Clarke *et al.* 1989a). This paper describes multiple, intensely developed, compressional deformational structures from the Anmatjira Range in the northern Arunta Inlier in order to place constraints on the tectonic evolution of the region.

*Present address: Department of Geology and Geophysics, University of Sydney, Sydney, NSW 2006, Australia.

Two Proterozoic tectonic cycles, defined by a sequence of repeated structural events, affected rocks in the Anmatjira Range (Fig. 1), each showing a progression from early reclined to later upright folding. The cycles are spatially restricted and temporally definable, and each was associated with low-P, high-T (LP–HT) metamorphism, culminating in a discrete granulite facies metamorphic (GFM) event, outlined by isograds (Fig. 1) and metamorphic overprinting criteria (Clarke *et al.* 1989a). These events have been dated by ion-probe U–Pb analysis of zircons (Collins *et al.* in press), confirming that each cycle was temporally separate.

To simplify the structural nomenclature, successive structural cycles are designated D_1, D_2, D_3 and separate fold and/or fabric forming events produced by progressive deformation during the one structural cycle are designated '*a, b, . . . n*' (e.g. D_{1a}, D_{1b} . . .,). We use the term 'terrane' to describe an area affected by different structural–metamorphic cycles (cf. Howell *et al.* 1985). Although the terranes are fault-bound, they also share a similar stratigraphy, which suggests they are para-autochthonous, rather than the allochthonous or 'suspect' terranes that have been involved in Cordilleran-style collision, as implied in the definition of Howell *et al.* (1985).

REGIONAL GEOLOGY

The Arunta Inlier is an extensive, multiply deformed and metamorphosed complex of Proterozoic age. A three-fold tectonostratigraphic subdivision was made by Stewart *et al.* (1984). The oldest 'Division One' rocks comprise mafic and felsic granofelses that are possibly metavolcanic, with minor psammopelites and calc-silicates. 'Division Two' rocks are mainly metasediments of turbiditic origin and 'Division Three' rocks are platform-style sediments that unconformably overlie the two other divisions. Granitoids have intruded all divisions, but are mainly seen in Division Two.

All assigned divisions crop out in the NW-trending Anmatjira Range and adjacent Reynolds Range. The granulite facies Weldon and Aileron metamorphics (Fig. 1) were both placed in Division One by Stewart (1981) and Warren & Stewart (1988). Division Two is represented by greenschist to amphibolite facies psammopelites of the Lander Rock beds (LRB), which are ubiquitous throughout the northern Arunta Inlier; they were locally metamorphosed up to granulite facies at Mt. Stafford (Stewart 1981, Vernon *et al.* 1990) and throughout the Anmatjira Range (Clarke *et al.* 1989a). The type-section for Division Three is in the Reynolds

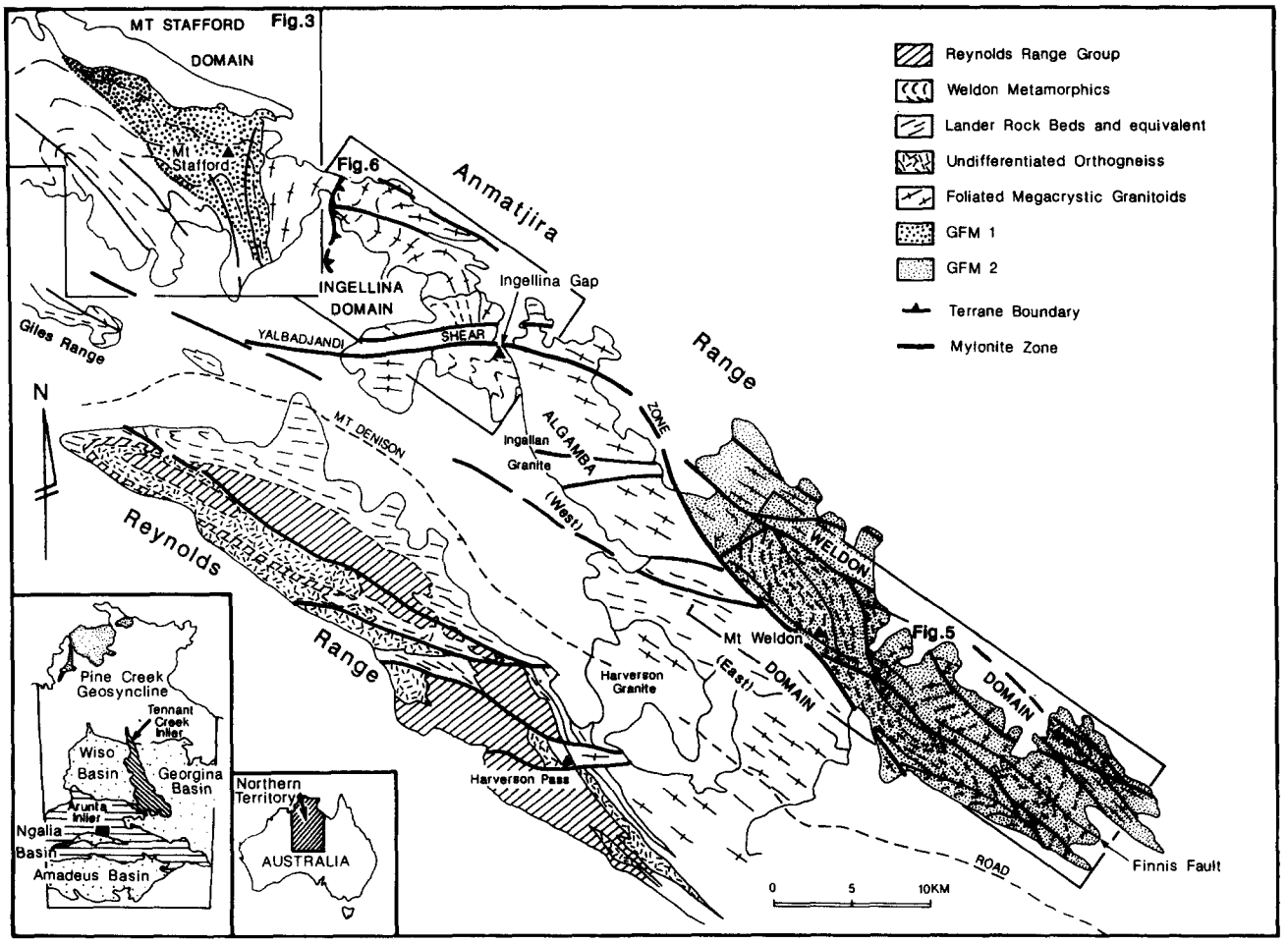

Fig. 1. Locality map of the Anmatjira and Anmatjira Range Region, Arunta Inlier, showing distribution of major rock types, areas of granulite facies metamorphism (GFM), and location of detailed maps (Figs. 3, 5 and 6).

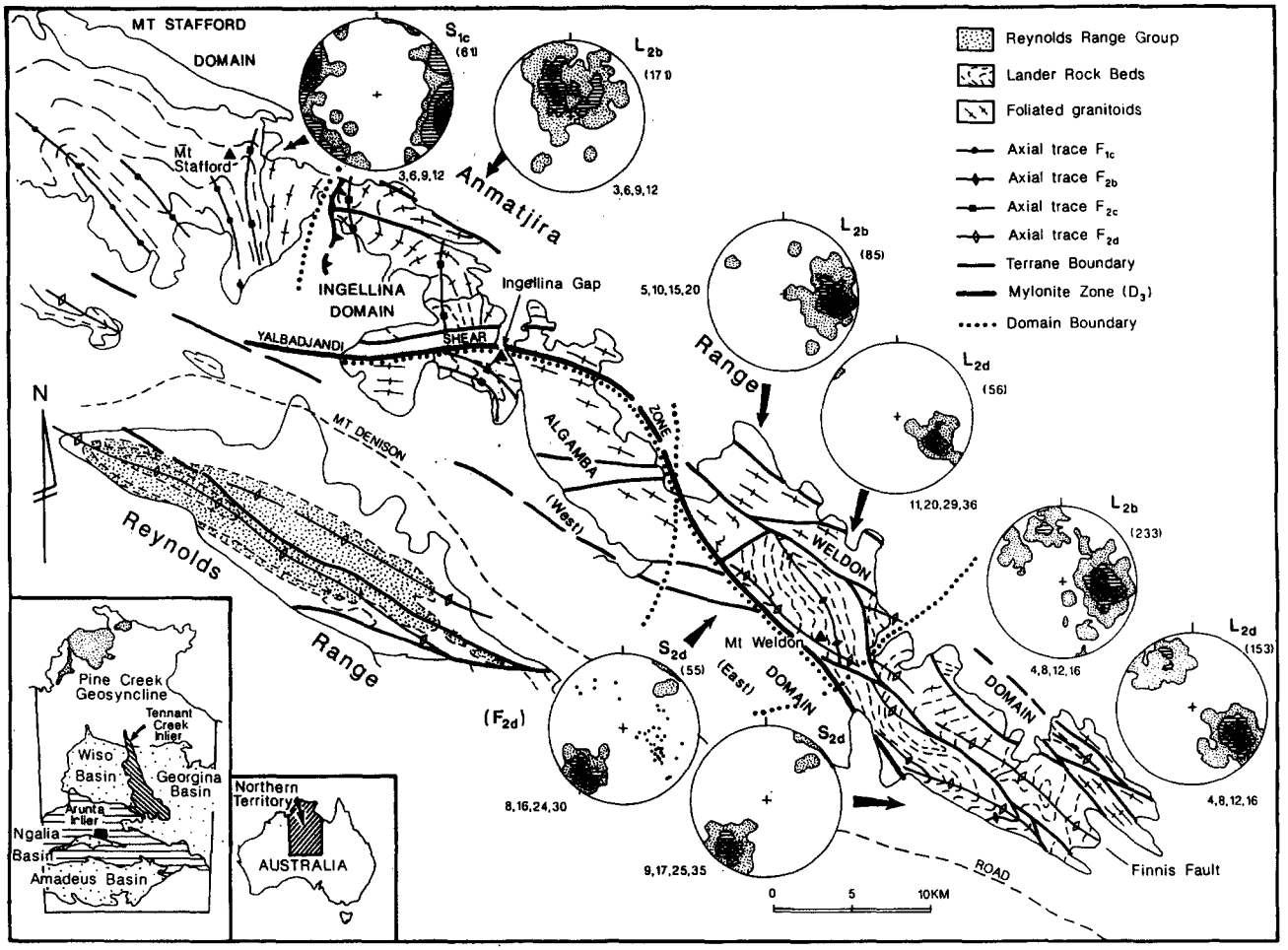

Fig. 2. Generalized structural map showing domain boundaries, axial traces of major folds and orientation data.

Range, where basal quartzites and metaconglomerates are conformable with carbonates and shales. All have been subjected to granulite facies metamorphism in the southeastern part of the range (Stewart 1981, Warren & Stewart 1988, Clarke & Powell 1990). The type sequence rests unconformably on LRB in the NW Reynolds Range (Stewart 1981), but further southeast at Harverson Pass and beyond, both divisions are conformable (Collins & Vernon 1987).

The range is subdivided into four broad structural domains (Fig. 2). The Mt. Stafford, Ingellina Gap and Mt. Weldon domains represent the northwest, central and southeast sections of the range. The Algamba domain, to the south of the range and separated from it by the Yalbadjandi shear zone, forms the valley between the Anmatjira and Reynolds ranges. The structural evolution of the Mt. Stafford domain is described first, followed by the Weldon and intervening Ingellina domains. Structures from the adjacent Algamba domain and Reynolds Range are also briefly discussed.

MT. STAFFORD DOMAIN

The Mt. Stafford domain (Fig. 3) comprises metapelites and metapsammites of the LRB, which are commonly well-bedded, although local, laterally persistent slump horizons also exist. Sedimentary structures, such as graded bedding and ripple cross-laminations, are uncommon but occur at all metamorphic grades and indicate that the sequence is generally right-way-up. The rocks are typically at muscovite grade, but show a spectacular metamorphic transition over a 10 km interval to peak GFM assemblages of cordierite–orthopyroxene–K-feldspar, indicating high-T (>700°C) at very low pressure of the order of 2.5 kb (Vernon *et al.* 1990). Undeformed migmatites are abundant at maximum grade (Vernon & Collins 1989). The metamorphic zones appear to form a regional aureole around large intrusive granitoid sheets, dated at 1820 Ma (Collins *et al.* in press).

D_1 *deformation*

Rocks of Mt. Stafford underwent three phases of deformation, ascribed to a single tectonic cycle (D_1: Table 1). Rare F_{1a} folds occur only in high-grade rocks where an axial planar S_{1a} foliation is defined by biotite and migmatitic segregations in pelitic gneisses. Locally, it is associated with boudinage (Fig. 4a). In some slump breccia zones, small (m-scale or less) sedimentary blocks are aligned in an asymmetrical pattern, suggesting W-directed transport, but a lack of lineations preclude definitive analysis. Nonetheless, F_{1a} folds show consist-

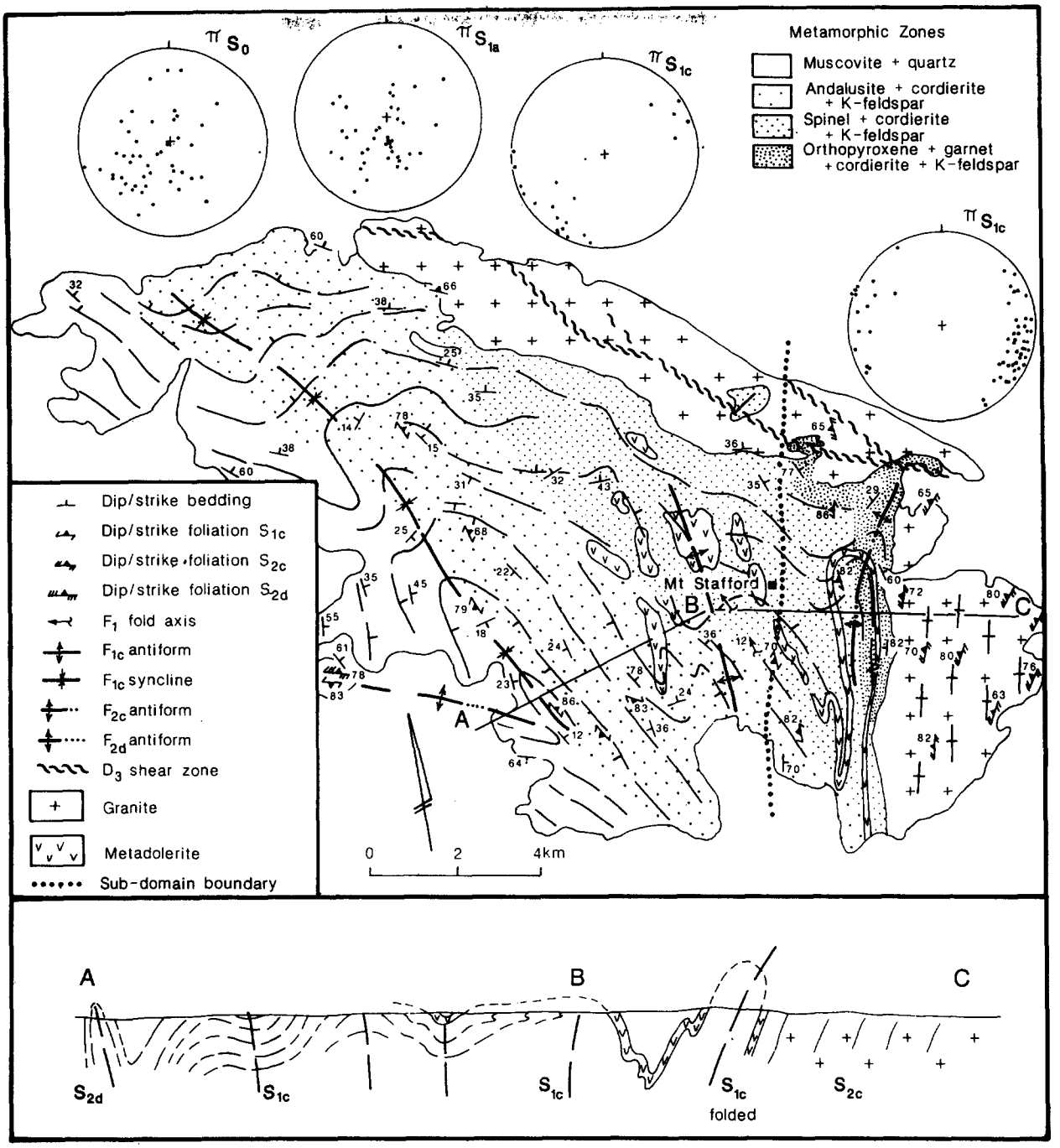

Fig. 3. Geology of the Mt. Stafford domain showing generalized structural trends (defined by S_0).

Table 1. Table of main structural events of the first tectonic cycle (D_1) in the Mt. Stafford domain

Mt. Stafford domain		
D_{1a}	D_{1b}	D_{1c}
F_{1a}	F_{1b}	F_{1c}
Metre-scale; close to tight; reclined to recumbent	Similar to F_{1a} but fold S_1; confined to high-grade rocks	Kilometre-scale; open to isoclinal; upright
S_{1a}	S_{1b}	S_{1c}
Not strongly developed; confined to high-grade rocks	Localized in fold hinges	Slaty cleavage in low-grade rocks; schistosity at higher grades; not developed in granulite facies rocks
L_{1a}		
Very weakly developed		

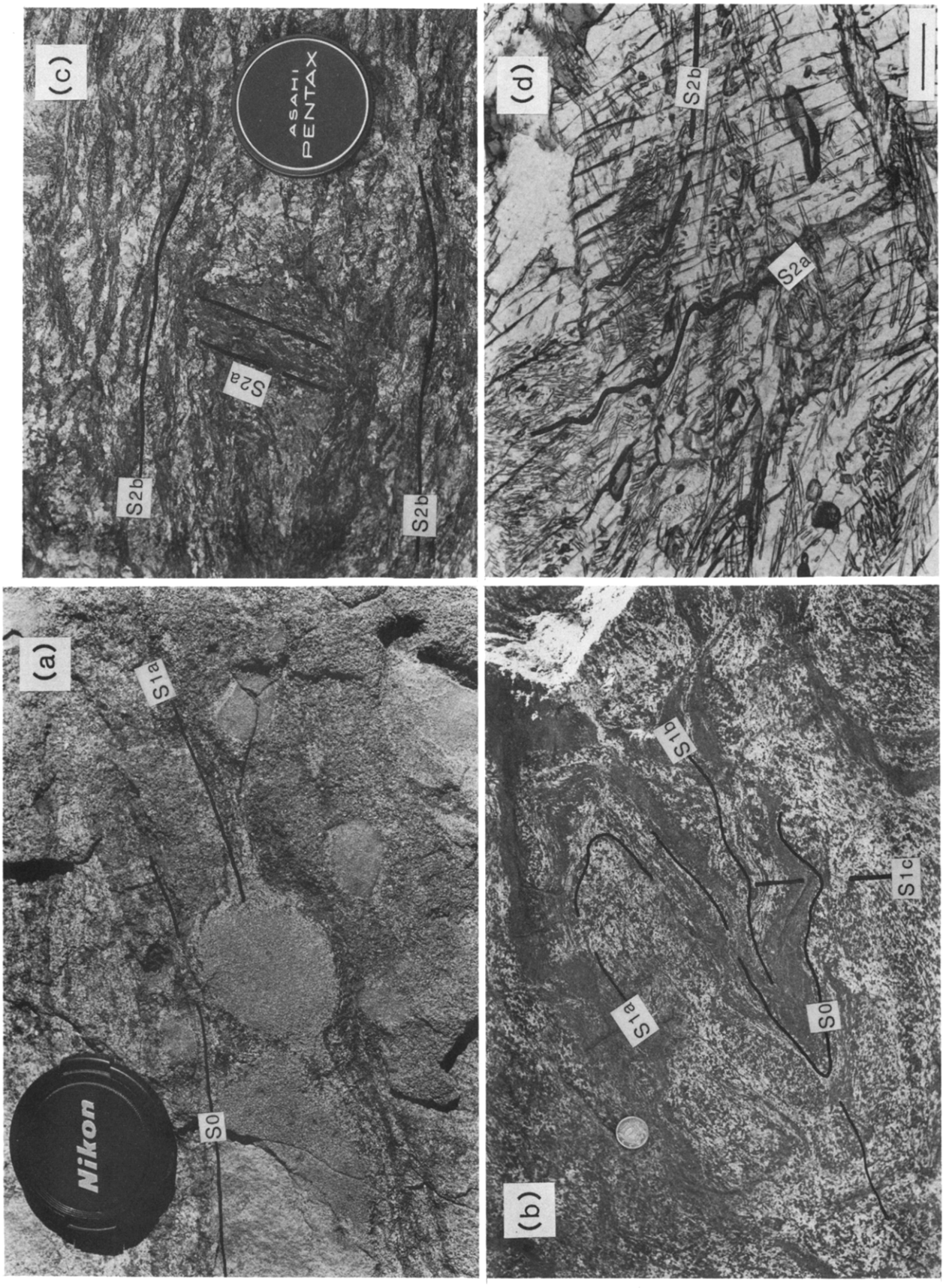

Fig. 4. (a) Boudinage of psammopelite. S_0 is drawn into the S_{1a} foliation in boudin necks; orthopyroxene–garnet–cordierite–K-feldspar zone, north of Mt. Stafford. Lens cap 5 cm diameter. (b) F_{1b} folds defined by S_{1a} and S_0 in migmatitic cordierite–spinel–K-feldspar gneisses, southeast of Mt. Stafford. Coin 23 mm diameter. (c) S_{2a} inclusion trails of sillimanite–biotite–quartz in garnet; migmatitic garnet–sillimanite gneiss, 2 km west of Mt. Weldon. Lens cap 5 cm diameter. (d) Photomicrograph of crenulated S_{2a} inclusion trails of sillimanite in garnet, forming 'herring-bone' structure, Weldon domain. Scale bar = 200 μm.

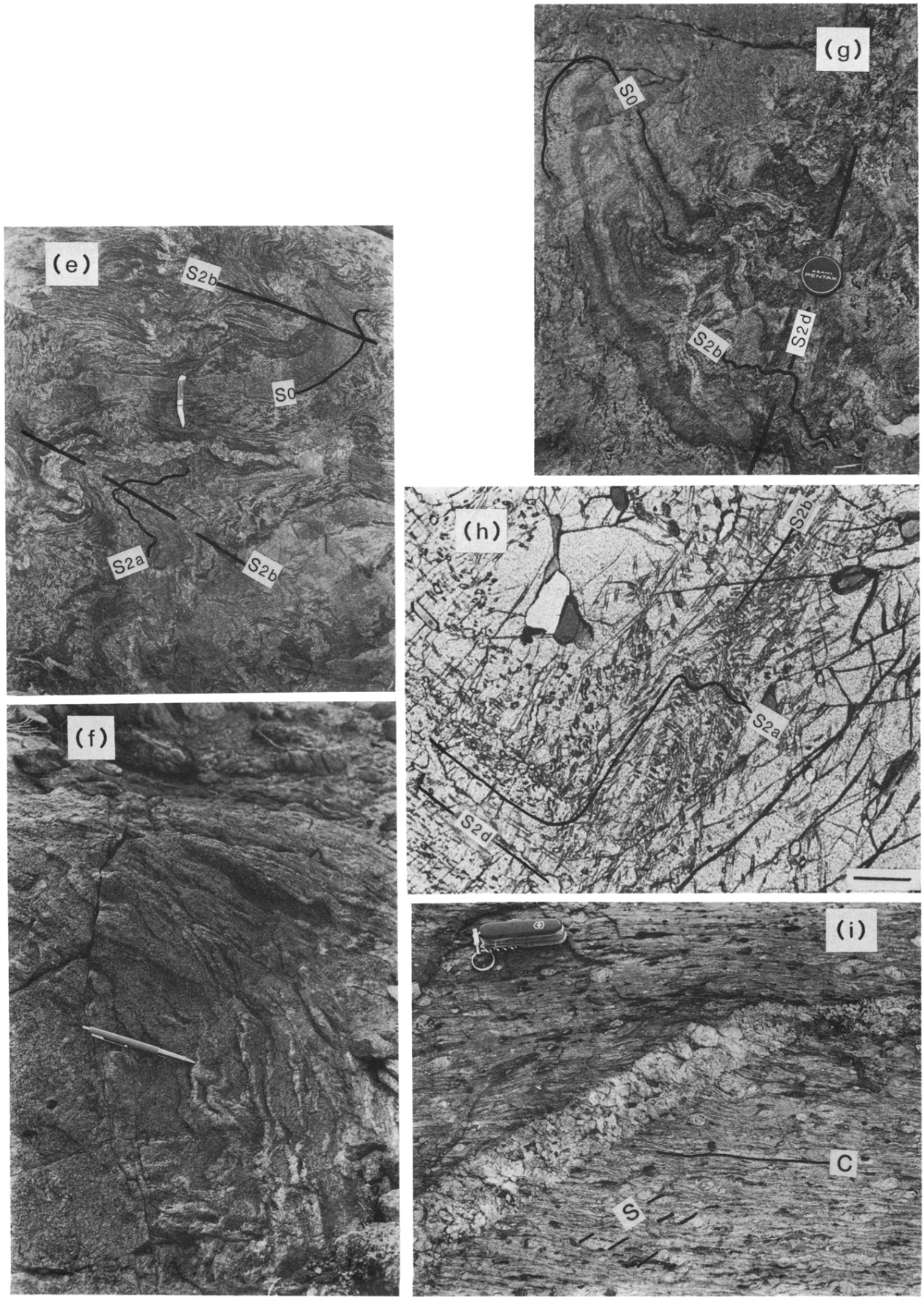

Fig. 4 (*continued*). (e) Recumbent F_{2b} folds in migmatitic cordierite–sillimanite gneisses, Weldon domain. Note folding of leucosome and S_{2a} in adjacent sillimanite-rich metapelitic layers. Knife 9 cm long. (f) F_{2b} sheath folds in quartzofeldspathic gneisses, Weldon domain. Pen (15 cm long) points to 'eye' of sheath fold. (g) F_{2b} folds refolded by inclined F_{2d}, southeast end of Anmatjira Range, Weldon domain. Lens cap 5 cm diameter. (h) Pelitic gneiss, Mt. Weldon, in which S_{2b} crenulates S_{2a}, but is itself folded into F_{2d} orientation. Scale bar = 200 μm. (i) High strain D_2 boundary fault between Mt. Stafford and Ingellina domains. Late-tectonic pegmatite suggests deformation and magmatism were synchronous.

ent asymmetry on a regional scale, irrespective of whether they are open to tight, and geopetal structures indicate inversion only on the short limb, which indicates transport in the direction of vergence (cf. Ramsay *et al.* 1983), which is westward.

S_{1a} is folded about W-verging recumbent folds (F_{1b}) in high-grade areas (Fig. 4b). These uncommon folds are absent from the lower grade rocks further west and we infer that the localization of subhorizontal foliations in the high-grade zones is due to mechanical weakening during high grade metamorphism (e.g. Weertman & Weertman 1975).

F_{1c} folds control the outcrop pattern and change progressively toward and through the zones of highest metamorphic grade (Fig. 3). From west to east, axial surfaces fan from NW- to N-trending; fold tightness changes from open to isoclinal and plunges change from subhorizontal and shallowly doubly-plunging to moderately steep (40–60°NE). S_{1c} also varies in style with metamorphic grade; in low-grade areas it is a slaty cleavage, but at higher grades it is a schistosity defined by cordierite–biotite or fine, cm-scale migmatitic leucosomes. S_{1c} is not developed in the highest grade gneisses, where F_{1c} folds merely rotate earlier fabrics.

D_2 *deformation*

F_{1c} folds have been reorientated into N–S attitudes at the eastern periphery of the Mt. Stafford domain. Progressive eastward tightening and tilting results in local overturning on F_{1c} fold limbs (Fig. 3). M_1 isograds are also folded and telescoped, so that they are most narrowly spaced in the SE. An axial planar foliation is locally strongly developed in granitoids to the east (Fig. 3), culminating as *S–C* fabrics (Berthé *et al.* 1979) in steep narrow mylonite zones that show both westward and eastward transport directions. The orientation of S_2 is parallel to the major thrust boundary of the Ingellina domain to the east (Figs. 1 and 2). The metamorphic response to loading during D_2 thrusting is the growth of sillimanite-bearing assemblages over andalusite porphyroblasts, indicating up-pressure conditions (Vernon *et al.* 1990).

WELDON DOMAIN

The Weldon domain (Fig. 5) comprises megacrystic granitoids on the northern side of the range and granulite facies rocks of the Weldon Metamorphics on the southern side, separated by the Finniss Fault (Fig. 1). A suite of orthopyroxene-bearing 'charnockitic' metagranitoids and mafic granofelses forms a distinctive subhorizontal marker unit in the Weldon Metamorphics (Fig. 5), which comprise a sequence of quartzofeldspathic gneisses, garnet–sillimanite migmatites, cordierite gneisses and minor cordierite-rich quartzites. Megacrystic granitoid sheets have intruded all rock types, but are dominant in the uppermost sections. On the north side of the range, where granitoids are abundant, xeno-

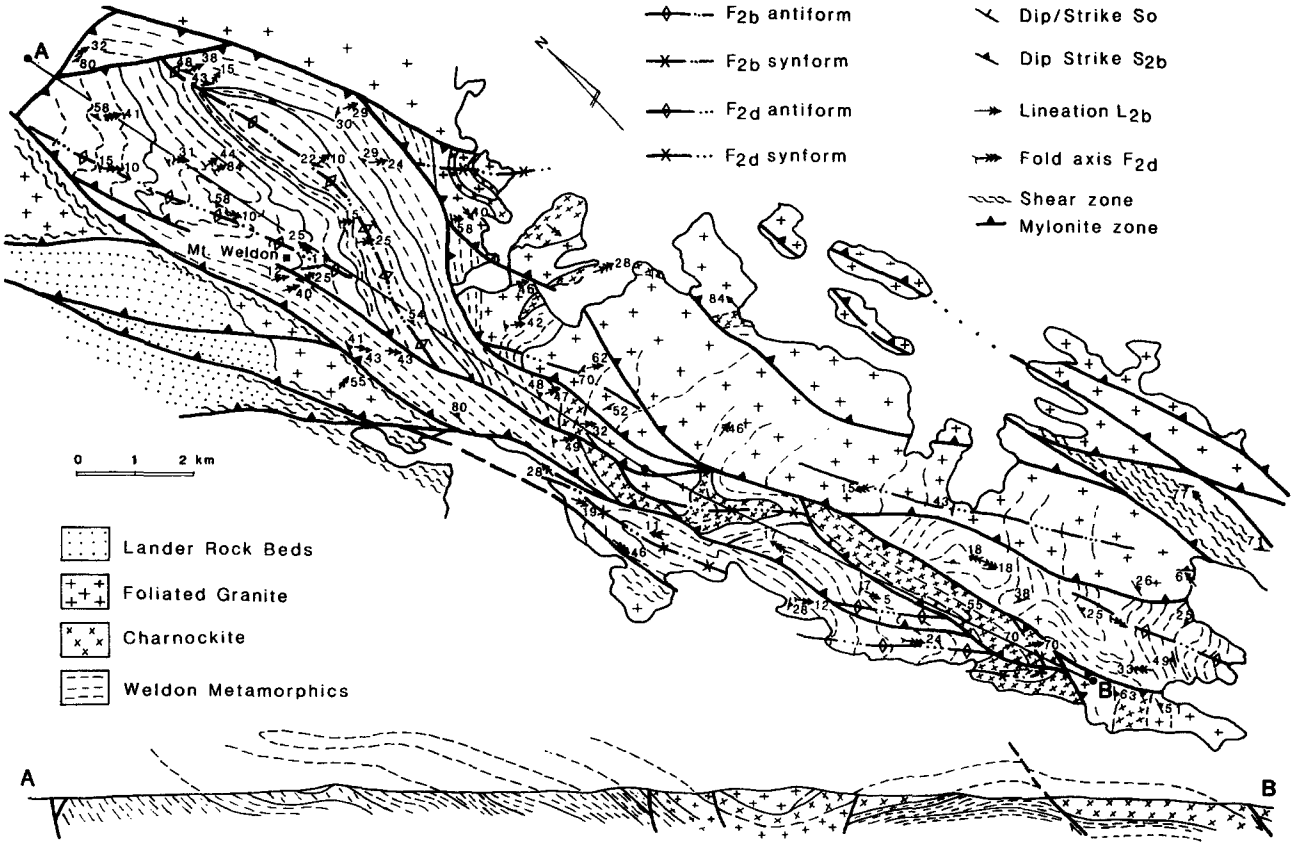

Fig. 5. Simplified geological map of the Weldon domain. Charnockite layer highlights the large-scale geometry of F_{2d} folds. Section A–B is located along F_{2d} axial trace to illustrate shallow-dipping orientation of S_{2b}.

Table 2. Table and correlation of main structural events of the second tectonic cycle (D_2) in the Weldon, Ingellina and Algamba domains (see text for discussion)

D_{2a}	D_{2b}	D_{2c}	D_{2d}
Weldon domain			
F_{2a}	F_{2b}		F_{2d}
Rare, isoclinal, intrafolial folds in mafic granofelses	m- to km-scale; tight to isoclinal; reclined to recumbent local sheath folds (Fig. 4f)		km-scale, upright open to tight NW–SE-trending
S_{2a}	S_{2b}		S_{2d}
Preserved as inclusion trails (Fig. 4c)	Strongly developed gneissosity; mylonitic in granites		Locally developed cm-scale crenulation cleavage
	L_{2b}		L_{2d}
	Strongly developed stretching lineation		Intersection and crenulation lineation in F_{2d} hinges
Ingellina domain			
	F_{2b}	F_{2c}	
	m- to km-scale; usually isoclinal, rare sheath folds	km-scale; open to tight; upright N–S-trending	
	S_{2b}	S_{2c}	
	Mylonitic in granites; usually reclined	Strong crenulation cleavage in schistose rocks. Local high-strain, mylonite zones	
	Strongly developed stretching lineation in high strain zones	Locally developed crenulation	
Algamba domain			
		F_{2c}	F_{2d}
		NNW-trending upright; open to tight; variable plunge (western area); absent to east	km-scale, E- SE-trending. Variable plunge. Open to tight
	S_{2b}?	S_{2c}	S_{2d}
	Low-grade layer parallel foliation to west. High-grade schistosity to east, mylonitic in granites	Slaty to spaced cleavage in western area	Weakly to strongly developed spaced cleavage. Local crenulation cleavage
	L_{2b}?		L_{2d}
	Local, strong extension lineation in eastern area		Local crenulation lineation; steep to shallow plunge

liths of the granofelses are common and vary from m- to km-scale. All were deformed during the D_2 tectonic cycle (Table 2).

Compositional layering (S_0) is defined by rhythmic alternation of high-grade minerals with granoblastic microstructure; it is commonly rotated parallel to an intense, composite shear foliation (S_{2b}), except in lower-strain zones where it is preserved in the hinges of F_2 folds.

D_2 *deformation*

F_{2a} structures are usually restricted to two-pyroxene granofelses, where they occur as isoclinal, intrafolial folds defined by migmatitic leucosomes. In other rock-types, F_{2a} folds are obliterated by later structures. S_{2a} is defined by sillimanite–biotite–quartz, and is commonly preserved as inclusion trails in garnet and/or cordierite (Figs. 4c & d).

The dominant structures in the Weldon domain were produced during D_{2b} deformation, including mesoscopic F_{2b} folds (Fig. 4e) and a strong foliation (S_{2b}), defined by aligned cordierite–sillimanite–garnet–biotite in pelitic gneisses and by an *S–C* mylonitic foliation (Berthé *et al.* 1979) in granitoids. A strong mineral rodding lineation (L_{2b}), defined by quartzofeldspathic aggregates and quartz ribbons in granites, is commonly dominant over S_{2b} in D_2 high-strain zones and produces *L*-tectonites.

F_{2b} fold axes show a variable relationship to L_{2b}. In high-strain zones, F_{2b} is parallel to L_{2b} and locally forms sheath folds (Fig. 4f), but in lower-strain zones, F_{2b} fold axes are usually curved and highly oblique to L_{2b}. Fold asymmetry suggests bulk westerly tectonic transport, consistent with S_{2b} *S–C* asymmetry in mylonitic granitoids. The observations indicate progressive, heterogeneous, non-coaxial strain during D_2 SW- to W-directed shear.

F_{2c} N–S-trending folds occur in the Ingellina domain (Fig. 2), but not in the Weldon domain. They predate

regional, shallow to doubly-plunging, NW–SE-trending folds (F_{2d}) seen throughout the Weldon domain and adjacent Reynolds Range.

F_{2d} folds become progressively tighter from north to south across the range, becoming locally isoclinal. At Mt. Weldon, an F_{2d} doubly-plunging antiform refolds an earlier reclined to recumbent major F_2 antiform (Fig. 5), which also occurs on a mesoscopic scale (Fig. 4g). The S_{2d} axial plane foliation is best developed in pelitic gneisses, defined by sillimanite–biotite enclosing porphyroblasts of M_2 cordierite and garnet (Fig. 4h). S_{2d} occurs in granitoids as cm-scale leucosomes that outline F_{2d} axial surfaces, or as a mesoscopic crenulation cleavage. An intersection lineation (L_{2d}) is also well developed, defined mainly by sillimanite–biotite. An L_{2d} crenulation lineation is the only D_{2d} structural element seen in mafic granofelses.

INGELLINA DOMAIN

The Ingellina domain, between Mts Stafford and Weldon, is best exposed near Ingellina Gap, north of the Yalbadjandi shear zone (Figs. 1 and 6). This region is dominated by intrusive granitoids that contain large xenoliths of metapelites. The rafts are remnants of LRB that have undergone several metamorphic events, characterized by (M_1) cordierite–K-feldspar assemblages overprinted by (M_2) sillimanite–biotite ± garnet assemblages (Clarke *et al.* 1989a), but the rocks record only two phases of deformation (Table 2).

D_1 *deformation*

The effects of the early deformation (D_1) are seen in the LRB xenoliths, which occur only near Ingellina Gap. Within the xenoliths, D_1 is evident as inclusion trails in elongate porphyroblasts of andalusite and K-feldspar, which have been enveloped by a penetrative foliation considered to be S_{2b}. The intensity of recrystallization during D_2 has obliterated most of the M_1–D_1 effects (Clarke *et al.* 1989a).

D_2 *deformation*

A well-developed biotite schistosity in LRB metapelites is concordant with a strong mylonitic fabric in the granitoids. The mylonitic foliation can be traced continuously from the Weldon domain and is therefore considered to be S_{2b}. *S–C* asymmetry and lineation orientation in D_{2b} mylonitic fabrics have been used to determine a sense of structural facing in the granites, which allows two types of F_2 folds to be distinguished. The asymmetry remains unchanged around some large fold closures south of Yalbadjandi Hill, suggesting that they are sheath folds (cf. Cobbold & Quinquis 1980) and therefore F_{2b}. Locally, S_{2b} is complexly folded about L_{2b}, producing *L*-tectonites. In contrast, a later set of

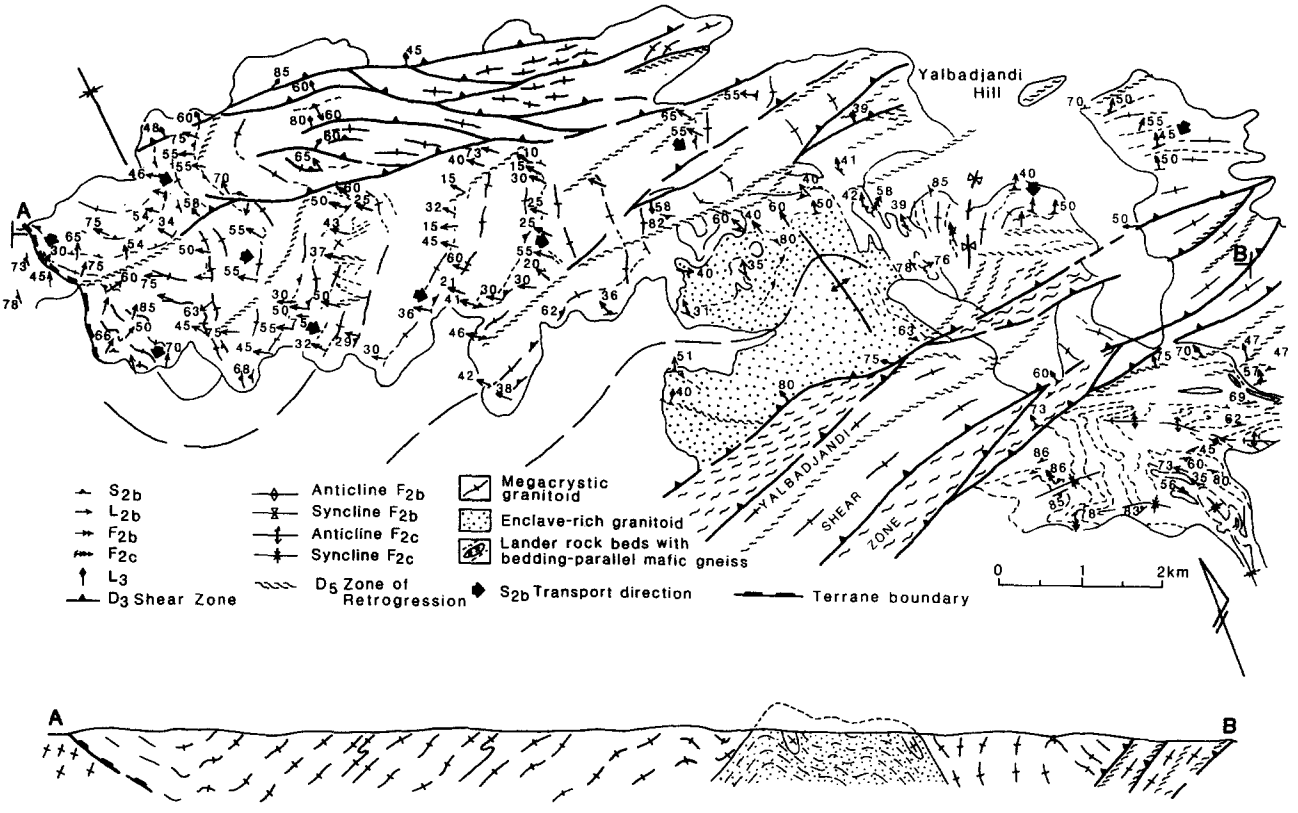

Fig. 6. Geology of the Ingellina domain. Note the systematic rotation of L_{2b} from west to east across macroscopic F_{2c} folds. On F_{2b} limbs (centre of map) S_{2b} is variable, but L_{2b} is relatively constant, typical of mylonitic fold development. See Fig. 1 for location.

macroscopic (F_{2c}) folds systematically reorient L_{2b} (Fig. 2) and S_{2b} (Fig. 6), indicating a macroscopic antiformal–synformal pair.

Parasitic folds in the schistose xenoliths in the major F_{2c} antiform (Fig. 6) trend N–S and plunge moderately (10–40°) to the NNW, similar to the plunge of the major synform to the west. A strong crenulation cleavage (S_{2b}), which strikes 160° and dips steeply NE, is developed in the schists, but an axial planar foliation is absent in the synform.

A high-strain shear zone, trending N–S, parallel to the F_{2c} axial trace, forms the western boundary of the domain. It is characterized by progressive rotation of S and C foliations into near-concordance (Fig. 4i) and by the localized development of L-tectonites. Strain patterns determined from the shape of mafic enclaves in granite, indicate that $X:Y:Z$ ratios reach 8:1:1, suggesting that constrictional strain locally developed. The zone dips eastward at 30–60° and S–C asymmetry clearly indicates reverse movement, requiring that the Ingellina domain has overridden the Mt. Stafford domain to the west.

ALGAMBA DOMAIN (WEST)

South of the Yalbadjandi shear zone (Figs. 1 and 6), multiply deformed, muscovite–quartz-bearing LRB are intruded by a weakly deformed granitoid, the Ingallan Granite, which extends continuously to the Weldon domain in the SE and forms the northern limit of the Algamba domain. The change from high- to low-grade metamorphic rocks across the shear zone, which separates the Ingellina and Algamba domains, is consistent with north-side-up movement as inferred from S–C asymmetry.

D_2 *deformation*

The earliest discernible foliation in the LRB is a layer parallel foliation defined by biotite–muscovite. Whether this foliation is related to D_1 or D_2 is unclear as it lacks a distinctive metamorphic assemblage; all foliations in this domain are defined by muscovite ± biotite and quartz. However, pseudomorphs of muscovite after andalusite were strongly flattened after retrogression, indicating an earlier metamorphism (M_1), presumably related to D_1. We therefore consider the layer-parallel foliation to be S_2, related to the strong fabric forming event, D_{2b} (Table 2). Furthermore, S_{2b} is folded into 100 m-scale upright folds (F_{2c}) that have a similar N–S trend to F_{2c} folds directly to the north in the Ingellina domain. These F_{2c} folds define the outcrop pattern of the LRB, as highlighted by a felsic amphibolite sill of metadiorite. F_{2c} fold axes vary considerably from subvertical through shallow to doubly-plunging, although the effect of later refolding on plunge attitudes is not well known.

F_{2c} structures are folded into open folds that produce km-scale Type 3 interference structures (Ramsay 1967). A disjunctive or spaced axial planar cleavage (S_{2d}) strikes generally E–W, dipping steeply northwards. The orientation is close to that of D_{2d} folds in the Weldon domain.

ALGAMBA DOMAIN (EAST)

South of the Yalbadjandi shear zone, near Mt. Weldon (Fig. 5), upper-amphibolite facies rocks of the LRB, containing sillimanite–muscovite assemblages, are intruded discordantly by megacrystic granites. M_2 metamorphic grade decreases rapidly southward from migmatitic schists to muscovite–biotite metapelites and metapsammites (Clarke *et al.* 1989a). Earlier (M_1) andalusite and K-feldspar porphyroblasts are pseudomorphed by M_2 sillimanite and muscovite, respectively. Structures in this domain are complicated by zones of extensive shearing and retrogression, which produced kyanite–muscovite–quartz in some late-formed pegmatites.

D_2 *deformation*

Directly south of Mt. Weldon, the LRB schists have a strong biotite–sillimanite foliation that strikes uniformly NW and dips moderately (~50°) NE. A strong sillimanite elongation lineation trends 060°, parallel to L_{2b} in the adjacent Weldon domain and therefore correlated with it (Table 2). To the south, megacrystic granites contain a flat-lying mylonitic foliation (S_{2b}), which progressively diminishes in intensity further south and the associated lineation also trends towards 060°. S–C asymmetry indicates SW-directed transport, consistent with the nature of S_{2b} elsewhere. These D_{2b} fabrics are gently folded about E–W-trending folds (F_{2d}). Several kilometers further to the SW, the S_{2b} foliation is not observable, but there is a very weak vertical NE–SW-trending foliation. This foliation can be traced westward through the Harverson Granite (Fig. 1), where it is associated with open folding of synplutonic granitic dykes. No evidence of the recumbent S_2 foliation exists in the Harverson Granite.

REGIONAL DEFORMATION

D_{2d} *deformation*

The only structures that appear correlatable across the Anmatjira and Reynolds ranges are NW–SE-trending, shallow- to doubly-plunging folds (Fig. 2), considered to relate to D_{2d} deformation (Table 1). In the Reynolds Range, F_{2d} folds are outlined by prominent basal quartzite units of the Division Three rocks (Figs. 1 and 2) and have been termed FII_2 folds by Dirks & Wilson (1990). S_{2d} is defined by a weak, biotite–sillimanite–cordierite foliation or by small, migmatitic leucosomes in F_{2d} hinges in GFM rocks at the southeast end of the range. To the northwest, S_{2d} is a slaty cleavage defined by muscovite, biotite and/or chlorite

alignment in upper greenschist–lower amphibolite facies rocks.

F_{2d} folds are also seen in the adjacent Giles Range (Figs. 1 and 2), and are similar to those of the NW Reynolds Range. They can be traced further northward into the Mt. Stafford domain, where gentle F_{1c} folds are tightened to steep orientations by F_{2d} folds (Fig. 3). There, the fold generations are generally coaxial with F_{1c} and can only be distinguished by overprinting criteria, namely, the folding of S_{1c} axial surfaces to produce a crenulation cleavage (S_{2d}).

D_3 *deformation (mylonite zones)*

The Anmatjira and Reynolds ranges are extensively transected by numerous greenschist and lower amphibolite facies shear zones that strike NW–SE, although less common zones branch E–W to form a macroscopic anastomosing pattern. In the Anmatjira Range, major E–W zones are spaced ~5 km apart and include the Yalbadjandi shear zone at Ingellina Gap. This zone separates the Mt. Stafford domain from the Giles Range in the west and the Weldon from the Algamba domain in the east (Fig. 1). It extends approximately 100 km along the south side of the Anmatjira Range and defines the southern limit of high grade rocks associated with M_1–D_1 and M_2–D_2. The mylonites have been regarded as Paleozoic in age by Collins & Teyssier (1989), but some may represent reactivated Proterozoic shear zones (Dirks & Wilson 1990).

D_3 shear zone development is more intense at the southeastern end of the Anmatjira Range, where ultramylonite and *S–C* mylonites zones are spaced only tens of meters apart. In the central part of the range, at Ingellina Gap, many mylonite zones dissipate northwestward into narrow branching zones that ultimately lose definition in the host granitoid (Fig. 6). Only the largest zones, spaced several kilometers apart, exist at the northwest end of the range.

The orientation of the shear zones varies systematically across the Weldon domain. To the south, the zones are N-dipping, and to the north they are S-dipping, indicating a fanning geometry. All zones show a strong down-dip lineation and reverse sense of movement, indicating a 'pop-up' structure (Collins & Teyssier 1989). The 'pop-up' terminates several kilometers north of Mt. Weldon, where major N- and S-dipping mylonite zones merge (Fig. 1).

DISCUSSION

Structural correlations, tectonic cycles and structural terranes

In the Mt. Stafford domain, early meter-scale, ductile shear zones and $F_{1a,1b}$ folds are poorly developed and are localized to areas of GFM. Early F_1 folds are reclined to recumbent, and tectonic transport direction was probably W-directed, based on $F_{1a,b}$ fold asymmetry and younging directions, but later (F_{1c}) are upright. The structural events constitute a single tectonic cycle, a conclusion supported by the same mineral assemblages defining all fold surfaces. The age is constrained by post-S_{1b}, pre-S_{1c} megacrystic granitoids, dated at 1820 Ma (Collins *et al.* in press).

The Weldon domain was also deformed during a single tectonic cycle. An early foliation (S_{2a}), preserved as inclusion trails in porphyroblasts, was largely obliterated during development of a penetrative, reclined to recumbent foliation (S_{2b}). L_{2b} stretching lineations and *S–C* asymmetry indicate dominant W-directed ductile shear during D_{2b} deformation. D_{2b} fabrics were folded into later upright F_{2c} and regional F_{2d} folds.

Although the Weldon and Ingellina domains are separated by an extensive area of alluvium (Fig. 1), similarities of rock-type, metamorphic grade and structural evolution suggest that they are a single terrane. Mylonite augen gneisses in both domains show consistent W- to SW-directed transport, considered to result from D_{2b} mylonitic deformation. Tectonic transport direction in the Algamba domain is also to the SW, as defined by D_{2b} mylonitic *S–C* fabrics in granitoids. Together, the three domains are considered to form a single structural entity, the Weldon terrane, extending some 60 km along the Anmatjira Range, and characterized by W- to SW-directed ductile shear.

Westward thrusting of the Weldon terrane during D_{2b} deformation has resulted in tectonic overriding of the Mt. Stafford domain on a 100 m to km-wide, E-dipping (30–60°), high-strain mylonite zone that shows clear reverse movement. Subsequent tectonic loading is consistent with metamorphic overprinting relationships in the Mt. Stafford domain, where poorly aligned sillimanite-bearing assemblages, pseudomorphous after andalusite, indicate an increase in pressure from 2.5 to 4 kb after D_{1c} deformation (Vernon *et al.* 1990).

The structural and metamorphic data indicate that the Mt. Stafford area is a separate entity from the Weldon terrane and has a distinctive tectonic cycle. U–Pb isotopic data from syntectonic D_{2b} charnockites in the Weldon terrane yield a 1760 Ma age (Collins *et al.* in press), and confirm that the Weldon terrane is much younger than the 1820 Ma tectonic cycle at Mt. Stafford. Thus, the structural, metamorphic and isotopic contrasts, the overprinting relations, and the major fault contact between the two areas, are sufficient criteria to define the latter as the Mt. Stafford terrane, according to the definition of Howell *et al.* (1985).

The regional NW–SE-trending folds, common to both terranes and to the Reynolds Range, were considered by Dirks & Wilson (1990) to be equivalent to F_{2b}, rather than F_{2d}. The subvertical axial surface of these folds (FII_2 of Dirks & Wilson 1990) was locally rotated into subhorizontal attitudes by ENE–WSW crenulation bands (FII_3) in the Reynolds Range, and Dirks & Wilson (1990) used this analogy to suggest that S_{2b} was originally subvertical in the Anmatjira Range. The present reclined to recumbent S_{2b} orientation in the latter would then result from FII_3 crenulation bands. Part of

the confusion appears to result from Dirks & Wilson (1990) equating S_0 in the Reynolds Range with the ($S_{2a,2b}$) foliations in the Anmatjira Range, which result from earlier intense deformation events. Also, if the NE–SW-trending folds in the Anmatjira Range are F_{2b}, the axial surfaces should be folded, but they consistently dip subvertically and strike NW–SE, indicating a later (F_{2d}) generation (Fig. 2). Thus, we contend that F_{2d} is correlatable between the two ranges, and that the effects of the D_2 tectonic cycle (*D*II of Dirks & Wilson 1990) were not identical.

Relationship of deformation to metamorphism

Zones of greatest structural complexity are associated with areas of highest metamorphic grade. In the Mt. Stafford terrane, at least two recumbent fold generations ($F_{1a,b}$) are evident in the granulite facies rocks, but in the lower grade rocks these structural elements diminish in intensity even though intervening major structural breaks do not exist and the enveloping S_0 surface is broadly horizontal (Fig. 3). Similar features are seen in the Algamba domain directly south of Mt. Weldon (Fig. 1), where metamorphic grade associated with M_2 decreases rapidly to the SSW (Clarke *et al.* 1989a) and D_{2b} fabrics in the granitoids are lost over a 5 km interval. To the southwest, only a weak S_{2d} foliation is observed in the older (1820 Ma) Harverson Granite (Fig. 1), which is metamorphosed only to muscovite–quartz grade (Clarke *et al.* 1989a). In contrast, the Possum Creek Charnockite, metamorphosed to granulite facies, shows evidence of multiple D_2 deformation and yet is considerably younger (~1760 Ma, Collins *et al.* in press). Thus, although D_2 strain might have been partitioned into discrete zones at lower grade, complex plastic deformation is restricted to areas of high-grade metamorphism, suggesting that the two processes are closely related.

Peak temperatures were reached prior to, or during, the earliest deformation event in each tectonic cycle (Clarke *et al.* 1989a, Vernon *et al.* 1990). In the Mt. Stafford terrane, wrapping of S_{1a} around andalusite suggests pre- to syn-S_{1a} prograde metamorphism, consistent with the presence of very small, random inclusions in cordierite which indicate a lack of foliation development before deformation. All structures in the high-grade rocks are delineated by high-grade minerals, indicating that the rocks were hot during *all* phases of D_1 deformation (Vernon *et al.* 1990). In the Weldon terrain, sillimanite–biotite inclusion trails (S_{2a}) in pre-S_{2b} garnet and cordierite porphyroblasts also indicate that the thermal peak was reached during the first deformation (D_{2a}) in that area (Clarke *et al.* 1989a).

Temperatures of 750–800°C occurring at mid- to upper-crustal depths (2.5–5.5 kb) indicate very high geothermal gradients during GFM and the sharp lateral metamorphic zonations suggest localized, transient heat sources, consistent with the fine-grained nature of many GFM rocks. The data suggest that the low-*P*, high-*T* (LP–HT) metamorphism was characterized by discrete, short-lived thermal pulses that were intimately associated with the tectonic cycles.

The regional metamorphic zonations are centred on granitoid intrusions. At Mt. Stafford, the zone of highest metamorphic grade is concordant with a 3 km-thick composite folded granite sheet that plunges to the northeast. The isograds, which exist on the southwest side (Fig. 3), occur below the sheet and define an inverted metamorphic isograd. Thus, the LP–HT metamorphism is a result of heating by granitoid intrusion. Localized hybrid zones of mixed felsic and mafic magmas exist at the base of the sheet, so some heat input is derived from mantle material, but it is minor. Similarly, the granite sheets of the Weldon terrain are concentrated in the zone of highest metamorphic grade, although no basal hybrid zones were found. Thus, the major source of heat for the thermal pulses was the granitoid sheets.

Given that the granites from both terranes are pre- and syn-tectonic, that the metamorphism is also pre- and syn-tectonic, and that deformation is most complex in the zones of highest metamorphic grade, it is clear that the thermal effects of granite intrusion and associated GFM influence the style and intensity of deformation.

Tectonic models

The association of deformation and early LP–HT metamorphism, and the induced anticlockwise *P–T–t* paths for both terranes (Clarke *et al.* 1989a, Vernon *et al.* 1990), is inconsistent with structural models that invoke continental collision to produce the early major reclined to recumbent folds. It may have resulted from extension, either of normal thickness crust (e.g. Wickham & Oxburgh 1985, Sandiford & Powell 1986, Buck *et al.* 1988) or of previously thickened crust, the thickening having been produced either by crustal shortening (Bell & Johnson 1989, Sandiford 1989) or magmatic overaccretion (Stüwe & Powell 1989b). In the Anmatjira Range, early-formed, high-*T* mineral assemblages occurring at mid-crustal depths (5–6 kb) do not indicate initial crustal overthickening, but more importantly, deformation is compatible with compression rather than extension. Kinematic indicators on the boundary fault confirm that the higher-grade Weldon terrane was thrust over the Mt. Stafford terrane, consistent with the late up-pressure metamorphic mineral assemblages in the latter (Vernon *et al.* 1990). Also, tectonic transport directions are invariably toward areas of lower metamorphic grade, rather than away from them, and upright folding continued during cooling of the terranes (Clarke *et al.* 1989a). Therefore, in the Anmatjira Range, LP–HT metamorphism was associated with thickening, rather than thinning of the crust.

Coeval LP–HT metamorphism and crustal thickening may be explained by contemporaneous mantle lithospheric thinning (Houseman *et al.* 1981, Loosveld & Etheridge 1990). In this model, crustal convergence produces a thickened mantle lithospheric root that becomes gravitationally unstable, detaches and sinks, allowing influx and underplating of the asthenosphere

onto the lower crust. To achieve the prograde andalusite–sillimanite assemblages typical of the Anmatjira Range GFM events, the model requires substantial crustal thickening (~60%), which must be reflected by a delay between the earlier stages of deformation and the onset of metamorphism. However, in the Anmatjira Range, the rocks were already undergoing peak thermal conditions during the earliest deformation.

Crustal thickening during LP–HT metamorphism, generating anticlockwise *P–T–t* paths, can be achieved by compression of a previously thinned crustal substrate, soon after heating of the terrane. Etheridge *et al.* (1987) appealed to crustal delamination, triggered by cooling of the lithospheric slab immediately after extension, to generate sufficient heat before deformation, whereas Thompson (1989) considered that heating would be a natural consequence of basin formation and sedimentation. Both models require that compression is a direct consequence of extension, and cannot explain the localized high-grade metamorphism in the Weldon terrane, 60 Ma after a similar episode in the Mt. Stafford terrane. A discrete thermal pulse is required, which is considered to be the intrusion of numerous granitoid (and minor mafic) sheets into the mid-crust.

Repeated intrusion of granite sheets into the mid-crust induces thermal softening in the high-grade, subhorizontal regional aureoles, and is facilitated by generation of fluids during metamorphism and migmatization. Plastic deformation is accelerated in these zones, a form of "melt-enhanced deformation" (Hollister & Crawford 1986), although the melts (and fluids) are considered to only reduce the yield strength of the host rocks, rather than lubricate the shear zones. Rheological contrasts between subconcordant granitoid sheets, incompetent migmatitic, and competent granofelsic layers, promotes subhorizontal ductile shear during compression and leads to complex deformation in the zones of highest metamorphic grade, centred on granitoid intrusions.

The model is similar to that proposed by Stüwe & Powell (1989a), but differs in two important aspects: (1) the thermal perturbation in the Stüwe & Powell model assumes conduction to be the dominant process, with passive behaviour of granites during intrusion; and (2) thickening directly follows extension, which implies the heat was associated with extension, rather than compression (Stüwe & Powell 1989a, p. 461). We consider that compression can occur anytime after extension, but it is the intrusion of granite sheets into the mid-crust that induces regional LP–HT metamorphism (cf. Hanson & Barton 1989), thermally softens it, and thereby localizes zones of complex deformation.

Early geological history of the Anmatjira Range

In Proterozoic northern Australia, the earliest rocks are typically rift-fill sediments deposited during extension of pre-existing, possibly Archaean, continental crust (Etheridge *et al.* 1987). In the northern Arunta Inlier, these sediments are represented by the LRB, which probably formed at ~1880–1870 Ma, based on lithological correlations with the Warramunga Group in the adjacent Tennant Creek Inlier (Blake & Page 1988) and U–Pb ages of individual zircon grains from the LRB (work in progress). Thus, the age of initial thinning of the crust is considered to be ~1880–1870 Ma (Fig. 7a). D_1 and D_2 tectonic cycles followed approximately 60 and 120 Ma later, at 1820 Ma in the Mt. Stafford terrane and at 1760 Ma in the Weldon terrane (Collins *et al.* in press). The cycles required discrete thermal pulses separate from that associated with basin formation, as extensional events usually take only several tens of Ma to cool (McKenzie 1978, Loosveld & Etheridge 1990).

The discrete thermal pulse associated with emplacement of a composite ~3 km-thick granite sheet in the Mt. Stafford terrane, induced a localized tectonic cycle (D_1). The 'regional aureole' (cf. White *et al.* 1974) around the granite sheet shows a dramatic decrease in metamorphic grade, reflecting a 75°C km^{-1} lateral gradient (Vernon *et al.* 1990). D_{1a} and D_{1b} structures are confined to the aureole and highlight the relation of deformation and metamorphism (Fig. 7b). However, km-scale F_{1c} folds extend beyond the aureole (Fig. 7c)

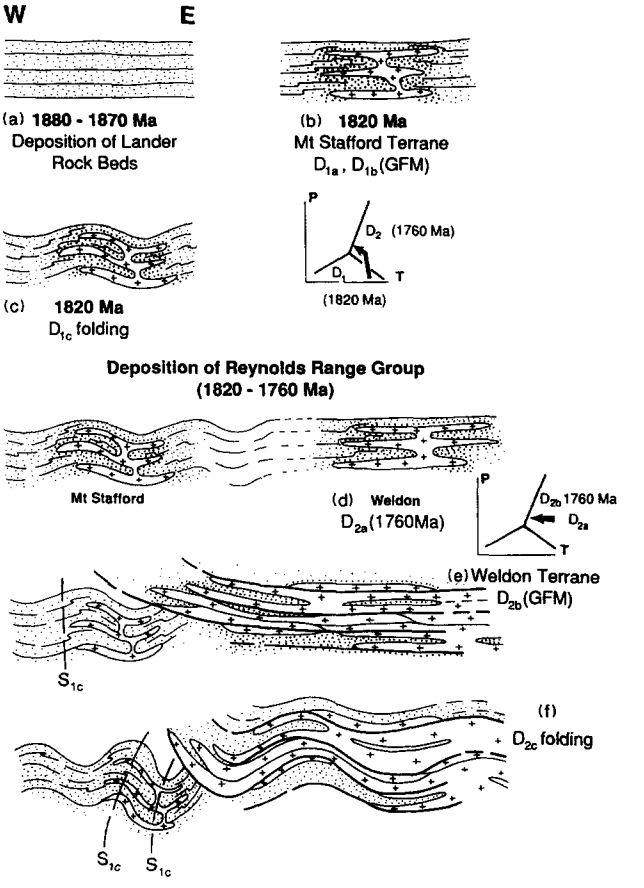

Fig. 7. Cross-section sketches showing evolution of the Mt. Stafford and Weldon terranes (1880–1760 Ma). The pressure increase from ~2.5 to 4 kb in the 1820 Ma Mt. Stafford terrane (Vernon *et al.* 1990) was caused by D_2 thrusting at 1760 Ma. Earliest assemblages in the Weldon terrane define S_{2a} and record peak temperatures before deformation began. Isobaric cooling ensued (Clarke *et al.* 1989a). See text for explanation.

and occur 10–15 km to the south in the Reynolds Range (Dirks & Wilson 1990), although they die out further southeast near Harverson Pass where the general 30–40° angular unconformity reduces to a paraconformity (Collins & Vernon 1987, Dirks & Wilson 1990). Apparently, thermal softening associated with granite-sheet intrusion at Mt. Stafford (Vernon *et al.* 1990) was sufficient to localize small-scale deformation during the first tectonic cycle (D_1), but not large-scale crustal deformation.

In contrast, the 1760 Ma GFM event in the Weldon terrane was associated with much more extensive sheet-like intrusion (Fig. 7d), and was widespread throughout the northern Arunta Inlier. It might also represent the GFM event in the Strangways Range, 100 km to the SE in the central Arunta Inlier (Warren 1983, Norman *et al.* 1989), also dated at 1760 Ma (Collins unpublished). Approximately 80% of the Weldon terrane comprises granite sheets of this age. This 1760 Ma tectono/magmatic event, characterized by early, large-scale, reclined to recumbent ductile shear associated with thrusting (Fig. 7e), was capable of substantially weakening the crust, thereby promoting complex regional compressional deformation. The tectonic cycle terminated with the generation of D_{2c} and D_{2d} upright folding (Fig. 7f).

CONCLUSIONS

Two distinct terranes are recognized in the Anmatjira Range, central Australia—the 1820 Ma Mt. Stafford terrane and the 1760 Ma Weldon terrane. Each terrane underwent a similar structural history of early recumbent folding and thrusting followed by upright folding, forming two discrete tectonic cycles. Deformation was intimately associated with LP–HT metamorphism in both terranes at mid-crustal levels, with the zones of highest metamorphic grade centered on granitoid intrusions.

Deformation began after heating and continued as each terrane began to cool, producing anticlockwise *P–T–t* paths. Complex deformation, characterized by ductile shear, was localized to regional aureoles around the granites, which were composed of numerous sheet-like bodies that occupy up to 80% of the terranes. The deformation is considered to result from thermal softening of the mid-crust, confined to areas of granitoid intrusion and surrounding regional aureoles, where magmatic and metamorphic fluids markedly reduce the yield strength of the rocks, thereby facilitating plastic deformation. The result is the production of discrete, complex structural terranes, characterized by anticlockwise *P–T–t* paths, and localized in zones of granite intrusion. A likely modern tectonic environment is the axis of a magmatic arc along an active continental margin.

Acknowledgements—Fieldwork for this project was supported by Australian Research Council Grant No. A38415716. We thank Christian Teyssier; Pat James and Tim Bell for critical reviews and Carol Simpson for improving the manuscript.

REFERENCES

Bell, T. H. & Johnson, S. E. 1989. Porphyroblast inclusion trails: the key to orogenesis. *J. metamorph. Geol.* **7**, 279–310.

Berthé, D., Choukroune, P. & Jegouzo, P. 1979. Orthogneiss, mylonite and noncoaxial deformation of granites; the example of the South-Amorican Shear Zone. *J. Struct. Geol.* **1**, 31–42.

Blake, D. H. & Page, R. W. 1988. The Proterozoic Davenport province, central Australia: regional geology and geochronology. *Precambrian Res.* **40/41**, 329–340.

Buck, W. R., Martinez, F., Steckler, M. S. & Cochran, J. R. 1988. Thermal consequences of lithospheric extension: pure and simple. *Tectonics* **7**, 213–234.

Clarke, G. L., Collins, W. J. & Vernon, R. H. 1989a. Successive early Proterozoic deformation and metamorphic events in the Anmatjira Range, central Australia. *J. metamorph. Geol.* **7**, 65–82.

Clarke, G. L., Guiriud, M., Powell, R. & Burg, J. P. 1987. Metamorphism in the Olary block, South Australia: compression with cooling in a Proterozoic fold belt. *J. metamorph. Geol.* **5**, 291–306.

Clarke, G. L., Powell, R. & Guiriud, M. 1989b. Low pressure facies metapelite assemblages and corona textures from McRobertson land, east Antarctica: the importance of Fe_2O_3 and TiO_2 in accounting for spinel bearing assemblages. *J. metamorph. Geol.* **7**, 323–336.

Clarke, G. L. & Powell, R. In press. Proterozoic granulite facies metamorphism in the southeastern Reynolds Range, central Australia: geological context, *P–T* path and overprinting relationships. *J. metamorph. Geol.* **9**.

Cobbold, P. R. & Quinquis, H. 1980. Development of sheath folds in shear regimes. *J. Struct. Geol.* **2**, 119–126.

Collins, W. J. & Teyssier, C. 1989. Crustal scale ductile fault systems in the Arunta Inlier, central Australia. *Tectonophysics* **158**, 49–66.

Collins, W. J. & Vernon, R. H. 1987. Structural and metamorphic evolution of the Anmatjira–Reynolds Range regions, central Australia. In: *Arunta '87 S.G.T.S.G. Field Guide* **3**, F1–F7.

Collins, W. J., Williams, I. S. & Compston, W. In press. Discrete granulite facies events dated by the ion-probe method: northern Arunta Inlier, central Australia. *Contr. Miner. Petrol.*

Dirks, P. H. G. M. & Wilson, C. J. L. 1990. The geological evolution of the Reynolds Range, central Australia: evidence for three distinct structural/metamorphic cycles. *J. Struct. Geol.* **12**, 651–665.

Etheridge, M. A., Rutland, R. W. R. & Wyborn, L. A. I. 1987. Orogenesis and tectonic process in the early Proterozoic of northern Australia. In: *Precambrian Lithospheric Evolution* (edited by Kroner, A.). *Am. Geophys. Un. Geodyn. Ser.* **17**, 131–147.

Hanson, R. B. & Barton, M. D. 1989. Thermal development of low-pressure metamorphic belts: results from two-dimensional numerical models. *J. geophys. Res.* **94**, 10,363–10,377.

Hollister, L. S. & Crawford, M. L. 1986. Melt-enhanced deformation: a major tectonic process. *Geology* **14**, 558–561.

Houseman, G., McKenzie, D. & Molnar, P. 1981. Convective instability of a thermal boundary layer and its relevance for the thermal evolution of continental convergent belts. *J. geophys. Res.* **86**, 6115–6132.

Howell, D. R., Jones, D. L. & Schermer, E. R. 1985. Tectonostratigraphic terranes of the Circum-Pacific region. In: *Tectonostratigraphic Terranes of the Circum-Pacific Region* (edited by Howell, D. G.). Circum-Pacific Council for Energy & Mineral Resources. *Earth Sci. Ser.* **1**, 3–30.

Loosveld, R. J. H. & Etheridge, M. E. 1990. A model for low-pressure facies metamorphism during crustal thickening. *J. metamorph. Geol.* **8**, 257–267.

McKenzie, D. P. 1978. Some remarks on the development of sedimentary basins. *Earth Planet. Sci. Lett.* **40**, 25–32.

Moore, J. M., Davidson, A. & Baer, A. J. (Eds). 1986. The Grenville Province. *Spec. Pap. geol. Ass. Can.* **31**, 358.

Norman, A. R., Clarke, G. L. & Vernon, R. H. 1989. The tectonic history of the Strangways Orogenic Belt: a barometric response to late compression. *Geol. Soc. Aust. Abs. Ser.* **24**, 106–107.

Park, G. 1981. Origin of horizontal structure in Archaean high grade terranes. *Spec. Publ. geol. Soc. Aust.* **7**, 481–490.

Phillips, G. N. & Wall, V. J. 1981. Evaluation of prograde regional metamorphism metamorphic conditions: their implications for the heat source and water activity during metamorphism in the Willyama Complex, Broken Hill, Australia. *Bull. Soc. fr. Minér. Cristallogr.* **104**, 801–810.

Ramsay, J. G. 1967. *Folding and Fracturing of Rocks*. McGraw-Hill, New York.

Ramsay, J. G., Casey, M. & Kligfield, R. 1983. Role of shear in development of the Helvetic fold-thrust belt of Switzerland. *Geology* **11**, 439–442.

Sandiford, M. 1989. Horizontal structures in granulite terranes: A record of mountain building or mountain collapse? *Geology* **17**, 449–452.

Sandiford, M. & Powell, R. 1986. Deep crustal metamorphism during continental extension: modern and ancient examples. *Earth Planet. Sci. Lett.* **79**, 151–158.

Stewart, A. J. 1981. Reynolds Range Region, Northern Territory. 1:100,000 Map Commentary, BMR. Canberra, Australia.

Stewart, A. J., Shaw, R. D. & Black, L. P. 1984. The Arunta Inlier: a complex ensialic mobile belt in central Australia. Part 1: stratigraphy, correlations and origin. *Aust. J. Earth Sci.* **31**, 445–456.

Stüwe, K. & Powell, R. 1989a. Metamorphic evolution of the Bungar Hills, East Antarctica: evidence for substantial post-metamorphic peak compression with minimal cooling in a Proterozoic orogenic event. *J. metamorph. Geol.* **7**, 449–464.

Stüwe, K. & Powell, R. 1989b. Low-pressure granulite facies metamorphism in the Larsemann Hills area, East Antarctica; petrology and tectonic implications for the evolution of the Prydz Bay area. *J. metamorph. Geol.* **7**, 465–483.

Thompson, P. H. 1989. Moderate overthickening of thinned sialic crust and the origin of granitic magmatism and regional metamorphism in low-*P*, high-*T* terranes. *Geology* **17**, 520–523.

Vernon, R. H. & Collins, W. J. 1989. Igneous microstructures in migmatites. *Geology* **16**, 1126–1129.

Vernon, R. H., Clarke, G. L. & Collins, W. J. 1990. Mid-crustal granulite facies metamorphism: low-pressure metamorphism and melting, Mount Stafford, central Australia. In: *High-temperature Metamorphism and Crustal Anatexis* (edited by Ashworth, J. R. & Brown, M.). *Spec. Publ. Miner. Soc.* **2**, 272–319.

Warren, R. G. 1983. Metamorphic and tectonic evolution of granulites. Arunta Block, central Australia. *Nature* **305**, 300–303.

Warren, R. G. & Stewart, A. J. 1988. Isobaric cooling of Proterozoic high-temperature metamorphites in the northern Arunta Block, central Australia: implications for tectonic evolution. *Precambrian Res.* **40/41**, 175–198.

Weertman, J. & Weertman, J. R. 1975. High temperature creep of rock and mantle viscosity. *Annu. Rev. Earth & Planet. Sci.* **3**, 293–315.

White, A. J. R., Chappell, B. W. & Cleary, J. R. 1974. Geologic setting and emplacement of some Australian Paleozoic batholiths and implications for intrusion mechanisms. *Pacific Geol.* **8**, 159–171.

Wickham, S. M. & Oxburgh, E. R. 1985. Continental rifts as a setting for regional metamorphism. *Nature* **318**, 330–333.